ISSN (Print) 1226-1750
ISSN (Online) 2233-6656
Journal of Magnetics 18(2), 142-149 (2013) http://dx.doi.org/10.4283/JMAG.2013.18.2.142

Clinical Application of MRI in an Animal Bone Graft Model

Xiaochen Liu[1], Wenxiao Jia[1]*, Gele Jin[2], Hong Wang[1], Jingxu Ma[1], Yunling Wang[1], Yi Yang[2], and Wei Deng[2]

[1]*Medical Imaging Center, the Second Affiliated Hospital, Xinjiang Medical University, Urumqi 830000, China*
[2]*Department of Spine Surgery, the First Affiliated Hospital, Xinjiang Medical University, Urumqi 830000, China*

(Received 16 March 2013, Received in final form 14 May 2013, Accepted 15 May 2013)

We aim to monitor vascularization of early bone perfusion following rabbit lumbar intertransverse bone graft fusion surgery using magnetic resonance imaging assessment. Correlation with graft survival status was evaluated by histological method. Experimental animals were randomly divided into three groups and the model was established by operating bilateral lumbar intertransverse bone graft with different types of bone graft substitute material. The lumbar intertransverse area of three groups of rabbits was scanned via MRI. In addition, histological examinations were performed at the 6th week after surgery and the quantitative analysis of the osteogenesis in different grafted area was carried out by an image analysis system. The MRI technique can be used for early postoperative evaluation of vascularized bone graft perfusion after transplantation of different bone materials, whereas histological examination allows direct visualization of the osteogenesis process.

Keywords : magnetic resonance imaging, bone graft, vascularization, histology

1. Introduction

Spinal fusion, which is of great importance in the applications of spine surgery, is an effective method in clinical orthopaedics for treatment of spinal cord injury, vertebral tumors, spinal deformity, spinal tuberculosis and degenerative bone diseases. Long-term practices and substantial research in clinical orthopaedics have proved that the optimal pathway to achieve effective spinal fusion of bone defects is to promote the local bone formation while connecting the corresponding spinal segments. Therefore, the bone grafting techniques have been commonly and more frequently used in clinical orthopaedics [1].

After transplantation, the bone graft must undergo three physico-chemical processes after transplantation, i.e., angiogenesis, bone regeneration and endplate bone fusion. Of these, the establishment of sound vascularization between the bone graft and the receiving area is the most important step [2]. After the graft is implanted into the body, the repair of bone defects must rely on vascularization which insures supply adequate blood to bone graft. Otherwise, it may easily lose viability due to lack of sound blood supply, and then become a foreign substance in the implanted body, which results in increasing the risk of strong rejection. Thus vascularization plays an essential role in repairing bone tissues. Therefore, to monitor whether the bone graft can rapidly vascularize after transplantation has become a hot spot of relevant research in recent years.

Tissue-engineered bone has shown potential in bone grafting, and vascularization of tissue-engineered bone is the basis and key for its survival and biological effectiveness [3]. Presently, ideal methods have been lacking for monitoring this process [4]. In order to identify a monitoring method for an early, noninvasive, dynamic evaluation of graft survival, in this study, in this study we try to monitor early vascularization of the tissue-engineered bone graft using the magnetic resonance imaging (MRI) technique and evaluate bone graft survival using histological method.

2. Materials and Methods

2.1. Laboratory animals and model establishment

2.1.1. Laboratory animals

The study protocol was approved by the ethics committee of the Second Affiliated Hospital, Xinjiang Medical University. A total of 30 healthy adult male New Zealand rabbits (2.8-3.5 kg) were provided by the Laboratory Animal Science Center, First Affiliated Hospital of Xin-

©The Korean Magnetics Society. All rights reserved.
*Corresponding author: Tel: +86-139-9925-5994
Fax: +86-21-6408-5875, e-mail: wenxiaojia126@126.com

© 2013 Journal of Magnetics

jiang Medical University. The rabbits were randomly divided into 3 groups based on the bone graft substitute materials: rhBMP-2/allogeneic bone (i.e., tissue-engineered bone) (group A), autologous bone (Derived from organisms of the selfsame individual) (B group), and allogeneic bone (Derived from individuals belonging to the same species but genetically dissimilar) (group C) (n = 10 each).

2.1.2. Model establishment

Hairs were removed from the surgical area using sodium thiosulfate 3 days prior to the surgery. The rabbits were injected in the ear vein with 3% pentobarbital sodium solution (30-35 mg/kg) for anesthesia, and then fixed in a decubitus position. The surgical area was disinfected using 2% iodophor solution. An incision was made along the rear midline to expose the bilateral ilium, and iliac bones ~20 mm × 15 mm in size were taken bilaterally. The incision was sutured after hemostasis. Thereafter, a longitudinal incision was made along the bilateral lumbodorsal fascia. The longissimus and multifidus were separated to expose the bilateral transverse fractures of L4 and L5. Complete hemostasis was performed after partial removal of the cortical bone. Composite bone, autogenous bone and allogeneic bone were implanted into the gap between the bilateral transverse fractures of the corresponding rabbit groups. Then, the muscle was covered and fixed, and the incision was sutured by layers and finally bandaged. Preoperative, intraoperative and postoperative use of penicillin (200,000 units) was via intramuscular injection, which was continued for 3 consecutive days thereafter. The rabbits were separately housed with free diet and movements.

2.2. MRI scan

2.2.1. Routine examination

Prior to the examination, the rabbits were injected in the ear vein with 10% ketamine (0.5 ml/kg) for anesthesia. Then, a Philips Gyroscan 1.5T MRI scanner was used to examine the rabbits. The rabbits were fixed in a prone position for scanning in a foot-to-head pattern using 8-channel head coil. A soft sandbag was placed underneath the rabbit body to adjust its position and ensure that the scanning parts fit the center of the coil. Dynamic contrast-enhanced MRI (DCE-MRI) was used for rabbit lumbar cross-sectional views and anatomical coronal scans (T1WI and T2WI) were also acquired. The scanning parameters were: 'TR 500 ms, TE 10 ms, THK 2.0 mm' (for T1) and 'TR 1171 ms, TE 110 ms, THK 2.0 mm' (for T2), respectively. Appropriate transverse fractures of L4 and L5 were selected for perfusion imaging.

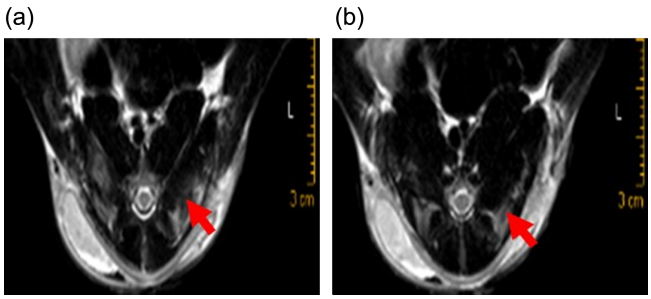

Fig. 1. (Color online) MRI T2WI images of group A rabbits. (a) 2 weeks after surgery, arrows indicate extensive high T2WI signal, apparently edema and inflammation; (b) 4 weeks after surgery, Arrows indicate T2WI signal is significantly decreased, the area of edema reduce, shows high sign Compared with 2th week after surgery, the operated area recovers slightly.

2.2.2. DCE-MRI scan

The middle cross-section of tissue-engineered bone was selected for perfusion imaging scan using fast low-angle shot sequences (TR 3.9 ms, TE 2.0 ms, FOV 320 mm, and slice thickness 2 mm) for 12 continuous dynamic scans in 6 min (each scan took 30 seconds). Then, the rabbits were injected in ear vein with contrast agent (Gadolinium diethylenetriamine pentaacetic acid, Gd-DTPA) using a Medrad spectris MRI injector (dose 1.5-2.0 mmol/kg; injection speed 1-2 mL/s). During scanning, the perfusion scan procedure was simultaneously initialized at the beginning of the bolus injection of contrast agent in order to obtain the dynamic image series (Fig. 1).

2.2.3. MRI imaging parameters

The original data were incorporated into the software package of Philips MRI system 2, 4 and 6 weeks after surgery. The grafted areas of three groups of rabbits were selected for comparative measurement using the statistical function of the MRI post-processing workstation. The region of interest (ROI) was selected at the layer showing the lesions with best quality and largest area. The ROI should be selected at a certain distance from the medial transverse fracture while avoiding the repeat region associated with the integration of bilateral transverse fracture and the bone graft. In addition, two surgeons were required to repeat the signal intensity measurements in the central grafted area of each group using the blinding method. In this study, the middle cross-section of tissue-engineered bone was used as the ROI. The signal intensity (SI)–time (T) curve automatically generated by a computer described the variations in signal intensity

before and after the enhancement and accurately reflected the characteristics of blood flow dynamics in the grafted area. According to the parameters in the curve, this study primarily focused on the dynamic monitoring of signal intensity increasing value SI and maximum linear slope value SS_{max}. The SI was calculated as follows:

$$SI\ (\%) = (SIc - SI)/SI \times 100\%,$$

Where SI is the signal intensity of lesions before enhancement, and SIc is the signal intensity of lesions after enhancement. The SS_{max} was calculated as follows:

$$SS_{max} = (SIend - SIprior) \times 100\%/[\ SIprior \times (Tend - Tprior)]$$

Where SIprior and SIend respectively represent the starting point of rapid increases and the maximum signal

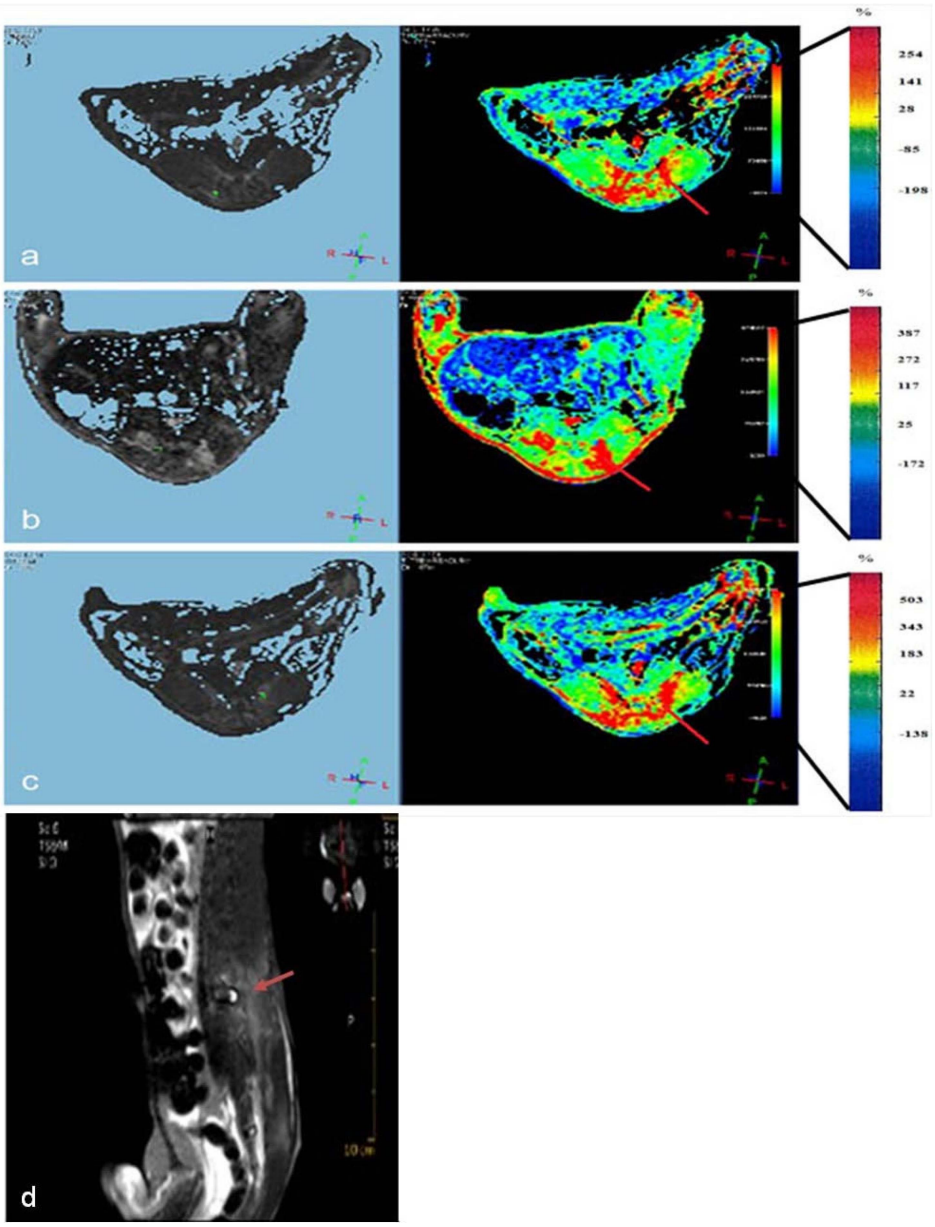

Fig. 2. (Color online) Perfusion (Percentage Increase of signal intensity; Unit: %/s) of group A over time after surgery (a) 2 weeks after surgery, the blood perfusion in ROI increasing in scattered point or piece style, as indicated by arrow, blood perfusion is increasing, shows high perfusion (Red), lower in Peripheral soft tissue (Yellow), low perfusion in Vertebral side water organization (Blue) (b) 4 weeks after surgery, arrow indicate that blood perfusion in ROI is higher compared to picture a, shows platy?? high perfusion (Red), low perfusion is shown in area of edema (blue). (c) 6 weeks after surgery, the high blood perfusion is in ROI, arrow indicate high perfusion area. (d) original MRI Sagittal positioning Image of Group A.

intensity in the SI–T curve, and Tprior and Tend respectively represent the time points corresponding to SIprior and SIend.

2.3. Histological examination and quantitative analysis

2.3.1. Histologicalmorphological examination

The rabbits were sacrificed at the 6th week after surgery and fused bone specimens were randomly taken from the lateral ilium for histological and morphological examination. 4 specimens including 8 fused bone blocks were collected from each group and the central parts were selected for electron microscopy. The specimens were prepared via fixation with 10% formalin solution, decalcification, dehydration at room temperature, immersion in wax, embedding with paraffin, sectioning into slices, and stained with hematoxylin and eosin.

2.3.2. Quantitative analysis

The prepared tissue sections were examined using a

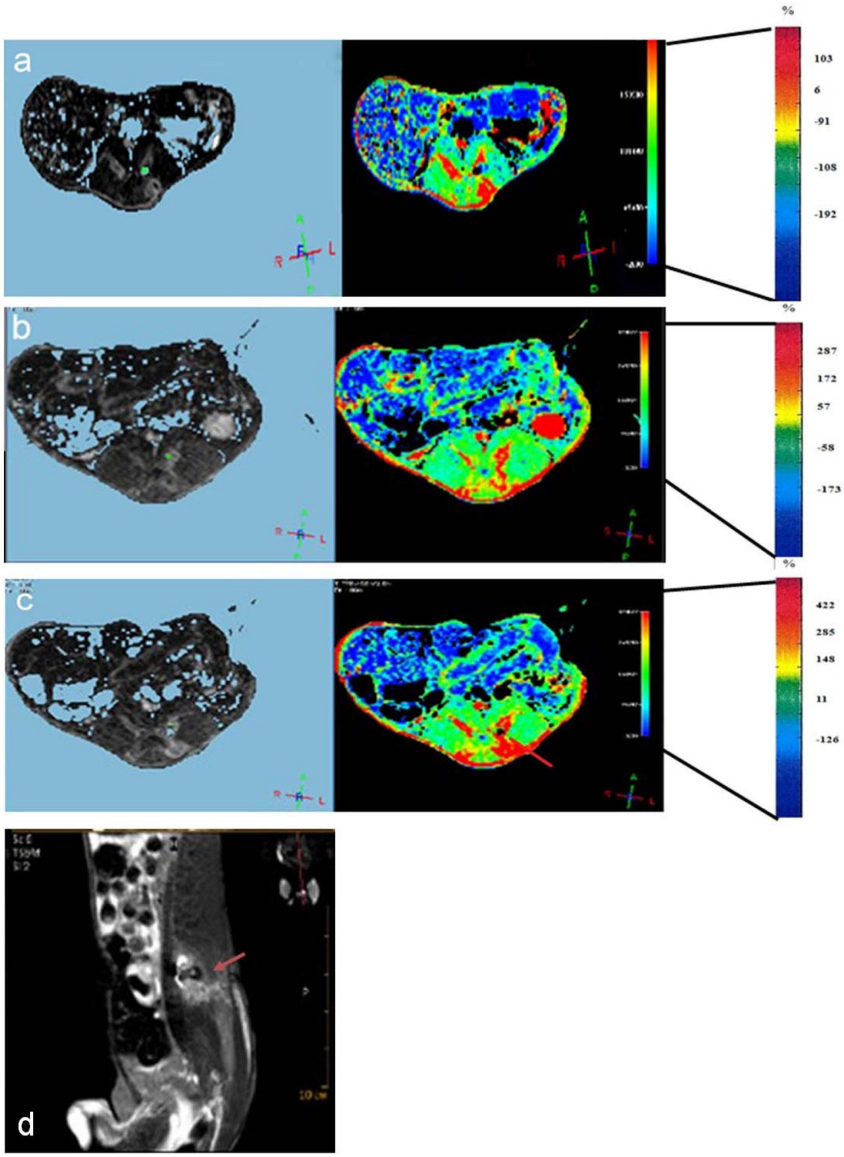

Fig. 3. (Color online) Perfusion (Percentage Increase of signal intensity; Unit: %/s) of autograft group rabbits over time (a) 2 weeks, there are no clear blood perfusion in ROI, as arrow indicate, there are patch-like blood stream in peripheral area of grafting bone (Red), compare to grafting bone, perfusion in peripheral soft tissue is lower (Yellow), low perfusion in edema and inflammation area (Blue). (b) 4 weeks, the blood increasing as strip-like in ROI, arrow indicate a high perfusion (Red), blood is reducing when blood supply is not enough (Yellow). (c) 6 weeks after surgery. Blood perfusion increase in band style, arrow indicate a high perfusion (Red), blood perfusion in peripheral area is lower than it is ROI (Yellow). (d) original MRI Sagittal positioning Image of Group B.

Leica LA automatic microscope equipped with a Pixera bood digital microscope camera and a Lecia Qwin V2.3 system for image analysis. Three groups of samples were taken from the same area and prepared as tissue sections for imaging under high magnification, with two regions randomly selected from the zone of ossification. The percentage of newborn bone tissue in the fused bone area among three bone groups was calculated by the image analysis software.

2.4. Statistical analysis

All data were statistically analyzed using the SPSS 17.0 statistical system. Multiple sets of data were analyzed using Analysis of Variance for repeated measurements (multiple comparisons by the LSD method), and expressed as the mean values ± standard deviation (Mean ± SD). $P < 0.05$ was considered statistically significant. For quantitative analysis of tissue sections, single factor analysis of variance was used, with $P < 0.05$ considered statistically significant.

3. Results

3.1. MRI examination

3.1.1. Conventional MRI scanning

The MRI-T2WI image in Figs. 1 showed manifestations of edema and inflammation in the surgical area after the posterior lumbar bone graft fusion surgery. Post-operative conventional MRI scanning of group A showed that the symptom of edema in the surgical area was alleviated at the 2th week after surgery, and the high signal intensity in and surrounding the surgical area slightly declined in the T2W1 image. After 4 weeks, the manifestations of edema were obviously alleviated in the T2W1 image, with substantially lower signal intensity compared with two weeks ago (Fig. 1).

3.1.2. DCE-MRI T1 perfusion imaging

As shown in Figs. 2 and 3, the DCE-MRI is advantageous in describing the dynamic changes of microvascular perfusion in rabbit lumbar intertransverse overtime. The perfusion also increased with time in the central grafted area in group A implanted with tissue-engineered bone and group B implanted with autogenous bone, as shown in Fig. 4. The perfusion was mainly surrounding the surgical area 2 weeks after surgery, and substantially enhanced in the grafted area after 6 weeks.

3.1.3. Comparison of ΔSI and SS_{max} among different groups

The ΔSI generally increased in the central grafted area

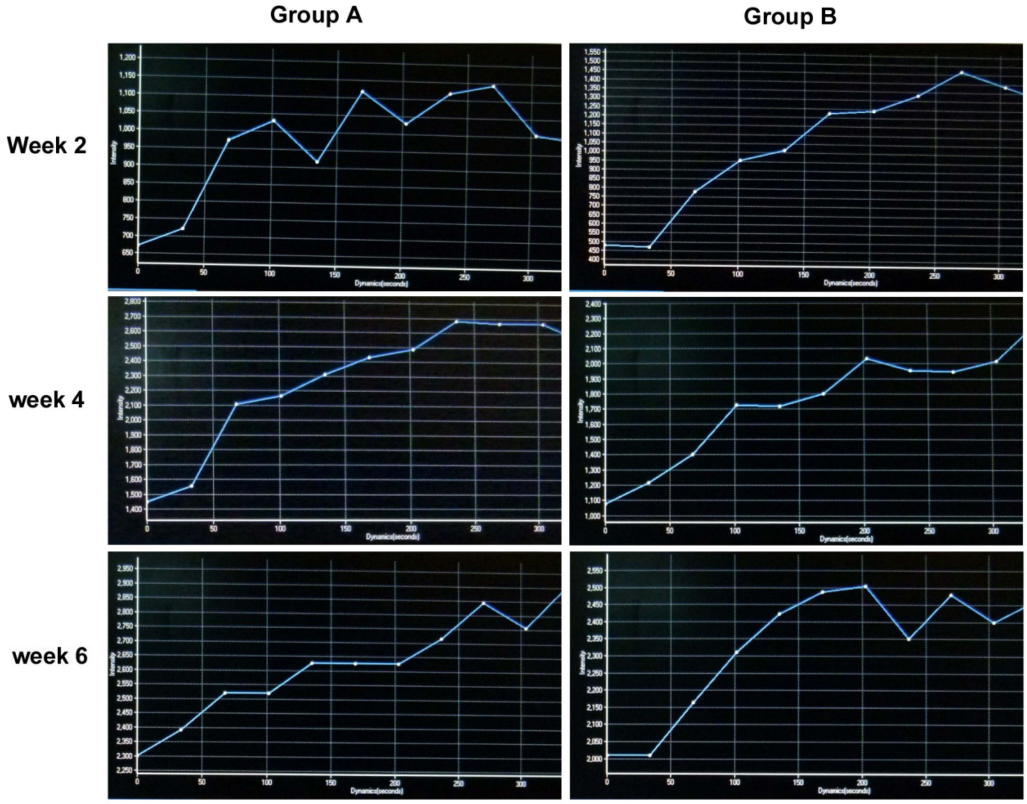

Fig. 4. (Color online) The perfusion curve monitoring of group A and B after 2, 4 and 6 weeks.

Table 1. Analysis of variance of the relative signal intensity increasing value SI of three rabbit groups 2, 4, and 6 weeks after surgery (Mean ± SD) (%/s).

Group	Row (N)	Central grafted area		
		2 weeks	4 weeks	6 weeks
A	10	26.06 ± 6.18^a	36.50 ± 8.25^a	40.02 ± 8.86^a
B	10	17.27 ± 4.21^b	28.45 ± 4.88^b	30.20 ± 5.94^b
C	10	7.23 ± 2.19^c	11.72 ± 2.36^c	14.16 ± 2.47^c

Note: [a]indicates significant differences between groups A and C, $P < 0.05$; [b]indicates significant differences between groups A and B, $P < 0.05$; and [c] indicates significant differences between groups B and C, $P < 0.05$.

of three rabbit groups 2, 4 and 6 weeks after surgery (statistically significant at 4 and 6 weeks, $P < 0.05$), and the maximum ΔSI occurred in group A after 6 weeks. Groups A and B had significantly higher ΔSI than group C after 2, 4 and 6 weeks. There were significant differences in ΔSI amongst groups, with largest differences observed after 6 weeks ($P < 0.05$) (Table 1). Regarding the SS_{max}, a similar increasing trend with time was observed in three groups 2, 4 and 6 weeks after surgery. Two weeks after surgery, there was significant difference in SS_{max} between groups A and C ($P < 0.001$) but not between groups A and B ($P > 0.05$). Four weeks after surgery, there were significant differences between groups A and B, as well as groups A and C ($P < 0.05$). Six weeks after surgery, there were significant differences between groups A and B ($P < 0.042$), as well as groups A and C ($P < 0.036$) (Table 2).

Table 2 Analysis of variance of the maximum linear slope value SS_{max} of three rabbit groups 2, 4, and 6 weeks after surgery (Mean±SD) (%/s).

Group	Row (N)	Central grafted area		
		2 weeks	4 weeks	6 weeks
A	10	13.65 ± 2.03^a	20.20 ± 1.76^a	24.45 ± 1.72^a
B	10	11.70 ± 2.10	15.61 ± 1.78^b	18.24 ± 1.44^b
C	10	8.12 ± 1.79^c	10.02 ± 2.11^c	14.55 ± 2.03^c

Note: [a]indicates significant differences between groups A and C, $P < 0.05$; [b]indicates significant differences between groups A and B, $P < 0.05$; and [c] indicates significant differences between groups B and C, $P < 0.05$.

3.2. Histological examination and quantitative analysis of tissue sections

3.2.1. Histological examination

Six weeks after surgery, substantial bone trabeculae occurred with a small amount of cortical bone observed in the tissue-engineered bone group, whereas few trabeculae and abundant woven bone were formed in the autograft group, and few trabeculae and abundant fibrous tissues were found in the allogeneic group (Fig. 5).

3.2.2. Quantitative analysis of histological sections

Compared with the allogeneic group, the area of newborn bone was substantially larger in the tissue-engineered bone group and autograft group ($P < 0.05$) (Table 3).

4. Discussion

4.1. Perfusion assessment via DCE-MRI

Vascularization plays a critical role in bone defect reparation, however, the postoperative trauma caused inflammation, hemorrhage and edema, leading to difficulties in separating the surgical area and the surrounding tissues within 1 week after the surgery. An effective diagnose method for monitor early vascularization after bone transplantation still not yet been explored. At present, the DCE-MRI technique is commonly used in clinical applications, such as differential diagnosis of tumors, musculoskeletal system and spinal joints [5-7]. DCE-MRI can be used to gain the parameters that reflect the microvascula-

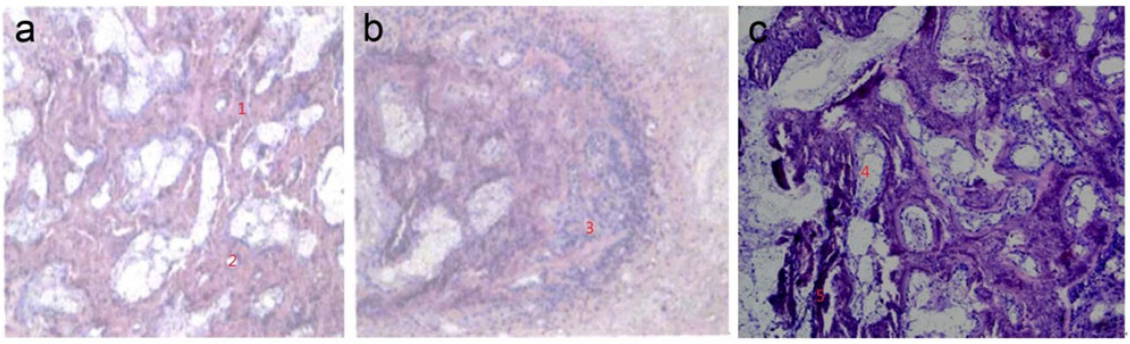

Fig. 5. (Color online) The histological picture. (a) Composite bone (×100), (b) Autologous bone (×100), (c) Allogeneic bone (×100). 1, bone trabecular; 2, haversian canal; 3, fibrous bone; 4, fibrillar connective tissue; 5, calcification.

Table 3. Quantitative analysis of tissue sections of three rabbit groups 6 weeks after surgery (Mean ± SD) (%/s).

Group	Row (N)	Central grafted area (%)
A	10	0.57 ± 0.08
B	10	0.52 ± 0.04
C	10	0.41 ± 0.06

ture of a tissue or tumor [6-13], such as microvasculature perfusion and capillary permeability, and mean transit time [Several compartmental models could also be used to fit these data (e.g., the bi-exponential Brix model), of them one could calculate the area under the curve (IAUC) as another measurement]. Nowadays, DCE-MRI is commonly used to assess bone graft viability [14, 15]. Thus, in this study we choose DCE-MRI to assess perfusion in bone grafting to visualize early vascularization.

4.2. DCE-MRI scanning layer and ROI selection

As the MRI technique is characterized by multi-faceted imaging, any cross-section of the grafted area can be used as the perfusion layer. The DCE-MRI can be performed on the cross-section, longitudinal section or coronal section, with TIC (Time Intensity Curve) curve automatically generated by a computer. To better observe the physiological changes in early graft vascularization, this study used the cross-section of grafted area for DCE-MRI scan and chose the target plane in the middle of rabbit L4 and L5 intertransverse bone graft. We carried out perfusion imaging and then followed by the ROI selection. Different ROI selections will cause variations in the results. Because the graft bone in this study is 1-1.5 cm in length and 0.2 cm in width, the ROI should be selected in the grafted area approximately 0.3-0.5 cm away from the medial margin of intertransverse bone graft. If the ROI was selected right in the grafted area showing the most obvious transverse process, it is likely to mistakenly (most probably due to partial volume effects, which could affect the authenticity) measure the bone graft and the lumbar intertransverse overlapped area as the ROI, resulting in biased changes in blood flow of grafted area.

The autologous bone has been considered to be the most effective graft material, and used as the "gold standard" for spinal fusion. However, in clinical practice, the amount of autologous bone that can be acquired is too small to repair the large bone defects. Therefore, the engineered artificial bone composite with growth factors which is characterized with good histocompatibility, osteoblast activity have received more attention in recent years, and some of them have been used as the autologous bone graft substitute. For example, the engineered artificial bone composite with recombinant human bone morphogenetic protein 2 (rhBMP-2), a soluble, low-molecular-weight transmembrane glycoprotein with a short half-life in the body, has began applied in the treatment of bone defects, nonunion and spinal fusion. In addition a large number of experiments have indicated that variety of carrier materials can facilitate the ostosis by slowing down the release rate of BMP-2, and maintaining its concentration in a local balance. The carrier material can be absorbed and degraded in a timely manner, thereby significantly improving the quality of osteoblast and accelerating the osteogenic process [16]. For example,the rhBMP-2/allogeneic bone complex has good biocompatibility, osteoconductivity and bone-inducing activity [17], thus can overcome the interference of local adverse mechanical factors and steadily release rhBMP-2 during bone repair or bone fusion, which have paved a new way for the repair of large segmental bone defect.

Imaging and histological results showed that 2, 4 and 6 weeks after surgery, the composite bone and autogenous bone showed higher metabolic activity and degree of revascularization than allogeneic bone, whereas 4 and 6 weeks after surgery, the composite bone seemed to have better metabolic activity and higher degree of revascularization than autogenous bone. In consideration of the literature, we suggest that rhBMP-2 is capable of inducing osteogenesis and angiogenesis across species contained in composite bone has been steadily released by the help of carriers materials. Despite lack of exogenous BMP-2, the autogenous bone prepared from fresh iliac bone contains a small amount of endogenous BMP-2 that contribute to the high blood supply and active metabolism through cooperation with BMP-7 and VEGF. As for the pre-treated allogenic bone, despite its excellent bone conduction, the growth factors that induce osteogenesis are primarily secreted from the injury site at an extremely low level, consequently, result in the blood supply and metabolism of allogenic bone were lower at different time points compared with the composite bone and autogenous bone. Some study [18] has shown that during the posterior lumbar interbody fusion surgery, rhBMP-2/allogenic composite bone yields higher/better or the same fusion effect, bone formation volume and osteoblast speed as autogenous bone. It suggested that the rhBMP-2/allogenic composite bone could be used as an alternative of autologous bone. Other research has shown that the rhBMP-2/allogenic tissue-engineered bone has excellent good osteoinductive activity, thus it is great advantageous to replace the autologous iliac bone graft [19]. In the rabbit posterior lumbar interbody fusion surgery, rhBMP-2/allogeneic composite bone can improve the bone formation and fusion rate,

thus it is an ideal alternative material of autologous bone [20]. Being a live artificial composite bone, tissue-engineered bone is a living bone graft, which can not only shorten the injury repairing time after surgery, but also improve the repairing quality of bone defects [21].

Acknowledgements

This work was supported by the National Natural Science Foundation of China (No. 30760257).

Conflict of Interest

The authors declare that they have no conflict of interest.

References

[1] E. E. Johnson, M. R. Urist, and G. A. Finerman, Clin. Orthop. Relat. Res. **250**, 234 (1990).
[2] X. M. Wang, G. X. Pei, D. Jin, K. H. Wei, C. Jiang, and G. H. Tang, Chin. J. Exp. Surg. **23**, 1510 (2006).
[3] D. Logeart-Avramoglou, F. Anagnostou, R. Bizios, and H. Petite, J. Cell Mol. Med. **9**, 72 (2005).
[4] R. E. Guldberg, Medical Devices & Surgical Technology Week. **20**, 350 (2005).
[5] A. R. Padhani and A. Dzik-Jurasz, Top Magn Reson Imaging **15**, 41 (2004).
[6] J. L. Montazel, M. Divine, E. Lepage, H. Kobeiter, S. Breil, and A. Rahmouni, Radiology **229**, 703 (2003).
[7] G. Brix, F. Kiessling, R. Lucht, S. Darai, K. Wasser, S. Delorme, and J. Griebel, Magn Reson Med. **52**, 420 (2004).
[8] S. B. Wedam, J. A. Low, S. X. Yang, C. K. Chow, P. Choyke, D. Danforth, S. M. Hewitt, A. Berman, S. M. Steinberg, D. J. Liewehr, J. Plehn, A. Doshi, D. Thomasson, N. McCarthy, H. Koeppen, M. Sherman, J. Zujewski, K. Camphausen, H. Chen, and S. M. Swain, J. Clin. Oncol. **24**, 769 (2006).
[9] A. C. Lockhart, M. L. Rothenberg, J. Dupont, W. Cooper, P. Chevalier, L. Sternas, G. Buzenet, E. Koehler, J. A. Sosman, L. H. Schwartz, D. H. Gultekin, J. A. Koutcher, E. F. Donnelly, R. Andal, I. Dancy, D. R. Spriggs, and W. P. Tew, J. Clin. Oncol. **28**, 207 (2010).
[10] M. K. Gule, Y. Chen, D. Sano, M. J. Frederick, G. Zhou, M. Zhao, Z. L. Milas, C. E. Galer, Y. C. Henderson, S. A. Jasser, D. L. Schwartz, J. A. Bankson, J. N. Myers, and S. Y. Lai, Clin. Cancer Res. **17**, 2281 (2011).
[11] C. S. van Rijswijk, M. J. Geirnaerdt, P. C. Hogendoorn, J. L. Peterse, F. van Coevorden, A. H. Taminiau, R. A. Tollenaar, B. B. Kroon, and J. L. Bloem, Eur. Radiol. **13**, 1849 (2003).
[12] J. P. Dyke, D. M. Panicek, J. H. Healey, P. A. Meyers, A. G. Huvos, L. H. Schwartz, H. T. Thaler, P. S. Tofts, R. Gorlick, J. A. Koutcher, and D. Ballon, Radiology **228**, 271 (2003).
[13] J. F. Meng, Y. C. Lv, and F. H. Lv, Chinese Journal of Radiology **35**, 578 (2001).
[14] N. Ehrhart, S. Kraft, D. Conover, R. N. Rosier, and E. M. Schwarz, Clin. Orthop. Relat. Res. **466**, 1897 (2008).
[15] Z. H. Dailiana, V. Zachos, S. Varitimidis, P. Papanagiotou, A. Karantanas, and K. N. Malizos, Eur. J. Radiol. **50**, 217 (2004).
[16] L. K. Cheung and L. W. Zheng, J. Craniofac. Surg. **17**, 100 (2006).
[17] S. S. Liao, K. Guan, Cui FZ, S. S. Shi, and T. S. Sun, Spine (Phila Pa 1976). **28**, 1954 (2003).
[18] J. K. Burkus, M.F Gornet, C. A. Dickman, and T. A. Zdeblick, J. Spinal. Disord. Tech. **15**, 337 (2002).
[19] S. D. Boden, J. Kang, H. Sandhu, and J. G. Heller, Spine (Phila Pa 1976). **27**, 2662 (2002).
[20] A. Minamide, T. Tamaki, M. Kawakami, H. Hashizume, M. Yoshida, and R. Sakata, Spine (Phila Pa 1976). **24**, 1863 (1999).
[21] C. A. Vacanti, W. Kim, J. Upton, D. Mooney, and J. P. Vacanti, Tissue Eng. **1**, 301 (1995).